Using laser-induced breakdown spectroscopy for the study of chloride diffusion in mortar and concrete

J. Mateo [a], M.C. García [b], A. Rodero [a],*

[a] *Department of Physics, University of Cordoba, Campus de Rabanales, Córdoba 14071, Spain*
[b] *Department of Applied Physics, University of Cordoba, Campus de Rabanales, Córdoba 14071, Spain*

ARTICLE INFO

ABSTRACT

In this work, the applicability of Laser-Induced Breakdown Spectroscopy (LIBS) for the analysis of chloride diffusion in mortar and concrete has been studied. The high resolution of this technique allows it to obtain a mapping of the chloride ions distribution in these materials upon being exposed to salted environments, thus providing an image of how chlorides diffuse inside them. The technique has been applied to mortar samples submerged in a salt-saturated solution for 3, 9, and 30 months. It has been demonstrated that the penetration profiles fit reasonably well Fick's second law in a modified version. The apparent diffusion coefficients for these samples were obtained ($D_{3months} = (5.94 \pm 0.05) \times 10^{-13}$ m^2/s; $D_{9months} = (3.6 \pm 0.6) \times 10^{-13}$ m^2/s; $D_{30months} = (2.1 \pm 0.8) \times 10^{-13}$ m^2/s). These results are in the range of the values found in other similar studies. The study of the evolution of these parameters over time revealed an age-factor $\alpha = 0.449 \pm 0.006$. Finally, LIBS was also applied to a concrete sample submitted to a long-period (60 months) immersion in the salt-saturated solution, giving similar good results ($D_{60months} = (1.81 \pm 0.03) \times 10^{-13}$ m^2/s), which demonstrates its suitability for the study of chloride diffusion in this type of material.

1. Introduction

The concrete industry is currently one of the engines of the economy worldwide, playing an outstanding role in the growth of modern societies and economies. Concrete is the most widely used construction material in the world. Its affordability, flexibility, and energy efficiency make concrete an obvious choice as construction material for infrastructure, including hospitals, schools, public buildings, and transport infrastructure. The global concrete market is estimated to grow from USD 792.2 billion in 2021 to reach up USD 1,374.2 billion in 2028 [1]. Guaranteeing the structural safety and durability of concrete buildings and infrastructure is of vital importance, and so is monitoring the concrete quality by detecting damages and determining their origin.

Long-term durability depends directly on the capacity of structures to resist the attack of the elements that cause their deterioration. These elements vary greatly depending on the location of the structures and their use. Structures located near the sea are particularly exposed to the action of chloride ions, which are one of the most harmful elements causing the degradation of reinforced concrete structures [2,3]. Either during the manufacturing process or by later exposure to external agents (including pollution, marine environments, or de-icing salts), can these

ions make it into the concrete. In reinforced concrete structures, chloride ions cause corrosion of reinforcing steel bars (rebars) through an electrochemical process that degrades (and ultimately destroys) the passivation layer protecting them [4–6].

Different mechanisms might cause the penetration of chloride ions into the matrix of concrete and mortar, including permeation (driven by a pressure gradient), absorption (driven by a moisture gradient), and diffusion (due to a concentration gradient). Permeation is a rare process in mortar and concrete, and absorption usually has an effect mainly on the surface layer, thus being usually diffusion the most outstanding mechanism bringing chloride ions to a significant depth in these materials.

When studying chloride diffusion in mortar and concrete, it must be considered that ions are moving through an inhomogeneous matrix containing a multitude of both solid and liquid components. It is a porous structure where diffusion takes place mostly through the pore and where a set of processes also affecting chloride transport occur in parallel. The pore structure greatly influences the rate of chloride penetration, and this structure depends on factors such as the water-cement ratio, the inclusion of additives in the mixture, or the hydration degree of the material [7,8]. Another process having an impact on

---

chloride ion penetration is the binding capacity of these ions, which partially react with the cement creating chemical bonds and eventually affecting the diffusion coefficient [9,10]. All this means that when we talk about the diffusion coefficient of chloride in mortar and concrete, we are referring to an effective diffusion coefficient that accounts for all these mechanisms ruling chloride transport.

Different prediction models for chloride ion diffusion have been developed, which analyze parameters such as the chloride binding effect [11], coupling effects of coarse aggregate and steel reinforcement [12], the compressive load applied to materials [13,14], and other features applying different diffusion acceleration conditions [15,16]. Most of these studies use a chemical method (Mohr method) to determine the chloride ion concentration in the samples. Occasionally, the analysis of the samples has been carried out by electrochemical methods such as impedance spectroscopy (IS), X-ray fluorescence (XRF), or energy-dispersive X-ray analysis (EDX). All these techniques are typically rated as destructive, as well as slow, and with poor spatial resolution. To address these drawbacks, in this work, we have shown that LIBS is a solid alternative to studying the chloride ion diffusion in the matrix of mortars and concrete. Moreover, it enables to carry out of quick and highly spatial resolved analyses, causing practically no damage to the sample, which could even be performed in situ if needed, so avoiding the transport of samples to the laboratory.

LIBS is an atomic emission spectroscopy technique that uses a high-energy laser to irradiate the surface of the sample under analysis. As a result, ablation occurs, and a part of the sample is vaporized. Electrons from the surface are accelerated by the action of the laser (due to the inverse bremsstrahlung effect), which triggers a set of collisional processes that eventually ignite a plasma containing sample species in an excited state. Shortly after the laser pulse ceases, this transient plasma extinguishes and excited species in it relax to their ground state while emitting optical radiation with wavelengths characteristic of each element present in the plasma.

LIBS technology is currently a well-established technique that allows the performing of a high number of elemental determinations regardless of the aggregation state of the sample [17–19]. Analysis can be performed in different ways, including a sole pulse or multiple pulses [20], either using a single laser or working with a double laser system [21–26]. Another advantage of using LIBS is the possibility of implementing it together with other techniques such as Spark Discharge (SD-LIBS), Molecular Laser-Induced Fluorescence (LIBS-MLIF), or Laser Ablation Inductively Coupled Plasma Mass Spectrometry (LA-ICP-MS-LIBS) [27–30]. The fields of application of LIBS greatly vary due to its ability to carry out fast and non-destructive analysis [31–33]. Thus, LIBS systems have been used in the study of archaeological samples, explosives analysis, environmental studies, forensic sciences, food industry, analysis of residues and nuclear waste, metallurgy, and mineral ore analysis [34–46], just to mention a few.

LIBS was first used for the analysis and diagnosis of building materials in the last decade of the 20th century. Its applications in this field include the determination of the distribution of salt in building materials through the study of sodium lines, the study of penetration in the carbonation process, and especially, the analysis of sulfates and chlorides in concrete [47–54], among others. The ability of this technique to perform surface mappings with high spatial resolution makes it a powerful tool for the study of the diffusion mechanism of chloride ions within the cement matrix in mortar and concrete, as we will show in this work.

In previous work, an optimized experimental set-up based on LIBS for the determination of chloride ion content in mortar samples was developed [55]. Optimization of all instrumental parameters, as well as environmental factors such as pressure and composition of the gas inside the chamber, was carefully carried out. In the present work, we investigated the use of LIBS as an alternative method to the study of chloride ion diffusion in the cement matrix of building materials by studying the chloride ion penetration in a set of samples previously submerged in

seawater. To the best of the authoŕs knowledge, there are not previous works using LIBS for this application. Thus, this study reveals for the first time the possibility of LIBS being used to perform chloride diffusion studies in construction materials and to determine the aging of these materials in salted environments.

Two different types of samples were analyzed, on the one hand, several mortar specimens subjected to multidirectional Cl⁻ penetration for various periods of time, and also a concrete sample subjected to unidirectional Cl⁻ penetration for a fixed period of time. After the immersion period, the samples were sliced crosswise and analyzed using LIBS, performing surface mapping at different sample depths. Thus, a set of penetration profiles were obtained and from them, details about the diffusion of liquid in the samples during their immersion were elucidated. Let us remark that the main aim of this work is to demonstrate the suitability of LIBS to obtain chloride ion diffusion parameters, rather than make a comprehensive study on chloride ion diffusion phenomenon in mortar and concrete samples.

2. Material and method

A schematic of the experimental set-up used in this work is shown in Fig. 1. It consisted of a 532 nm Nd:YAG pulsed laser of 320 mJ (generating radiation pulses 10 ns long at a 10 Hz repetition rate), and an optical lens system focusing the laser pulses into a vacuum chamber hosting the sample in a helium atmosphere. The light emitted by the sample upon laser irradiation was focused by another set of lenses onto the detection system, consisting of a spectrograph equipped with a grating of 1200 lines/mm and an intensified CCD, operating in conjunction with a digital delay generator (DDG).

The flow of gas through the chamber and the pressure inside it were controlled and kept within the optimal range obtained through calibration [55].

For the determination of the chloride ion content of the samples, the atomic line Cl I 837.60 nm was used [47–52,54]. Among Cl I lines detected, Cl I 837.60 nm was intense enough, was not overlapped with others, and did not experiment from self-absorption, which motivated its choice to measure the amount of chloride ion present in the sample. However, due to fluctuations between measurements (originated by little variations in the laser intensity, among other causes), when working with accumulations of measurements it is not possible to directly relate the intensity of the Cl I line to the concentration of chloride ions. This makes it necessary to relate the Cl I 837.60 nm line to
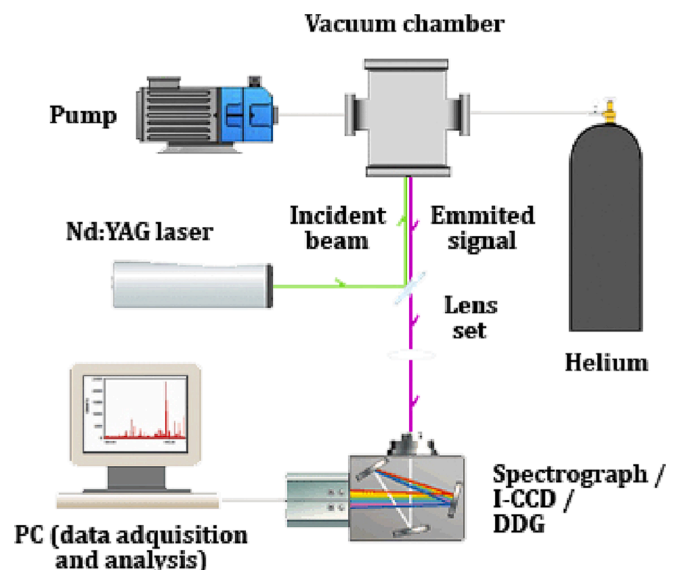

Fig. 1. Experimental set-up for LIBS analysis of samples.

another one serving as a reference, which remains constant and independent of the chloride ion concentration. It is also essential that the reference line is located close to the chlorine atomic line so that both lines can be covered within a single wavelength measurement window so that both can be measured at the same laser shot. All these requirements are fulfilled by Ca II 849.80 nm line, since this line intensity is characteristic of the type of cement used in the fabrication of the samples and is close enough to the Cl I line (Fig. 2). Thus, the chloride ion content of the sample will be determined by the ratio between the areas of the lines Cl I 837.60 nm and Ca II 849.80 nm [55].

2.1. Preparation of samples

For the study of the chloride ion diffusion, a set of mortar specimens of dimensions 40x40x160 mm^3 were prepared as described in EN 196–1:2005 standard [56]. This procedure entails the use of Portland CEM I 42.5R/SR cement (Table 1) and CEN standardized sand (grain size range of 0.08–2.00 mm). The resulting specimens were submerged in a saturated solution of sea salt for different periods of time (Table 2). The immersion was made by keeping the specimens completely exposed through all their faces so that the penetration of chloride ions took place from all directions (Fig. 3-A). Subsequently, the specimens were sliced perpendicular to their long axis into eight equal fragments 20 mm thick each, using a diamond blade cutter (Fig. 4-A), and the central fragments were used to perform the LIBS analysis. These fragments were dusted with dry air to avoid the removal of chlorides by washing.

For the study of the diffusion of chloride ions in concrete, a cylindrical specimen 150 mm in diameter and 300 mm in height was used. It was manufactured following the procedure described in EN 12390-2:2019 standard [57], using the same cement as utilized for mortar sample preparation, and a maximum thick aggregate size of 40 mm. This concrete specimen was covered with epoxy resin to protect it from chloride ion penetration, leaving only its upper face uncovered, and it was immersed in a saturated solution of sea salt for sixty months (Fig. 3-B). After this time, the sample was vertically sliced into two equal parts using a diamond blade cutter. A fragment of dimensions 40x40x20 mm^3 (similar to the mortar samples) was extracted from the top of one of these parts, so that one of the sides corresponds to the face of the original specimen exposed to the salt solution (Fig. 4-B), and was submitted to

Table 1
Composition of Portland CEM I 42.5R/SR cement.

	Cement characteristics	Usual	Standard
Components	Clinker (%)	95	95–100
	Limestone (L) (%)	5	–
	Setting regulator, "plaster" (%)	6	–
	Volatile ashes (V) (%)	–	–
	Pozzolana (P) (%)	–	–
	Steel slag (S) (%)	–	–
Chemical	Chlorides (Cl$^-$) (%)	0.01	0.10 max.
	Sulfur trioxide (SO$_3$) (%)	3.4	4 max.
	Loss by calcination (%)	3.1	5 max.
	Insoluble residue (%)	0.8	5 max.
Physical	Blaine specific surface area (cm^2/g)	3800	–
	Le Chatelier expansion (mm)	1	
	Setting start time (minutes)	130	60 min.
	End time of setting	170	–
Mechanical	1 day compression (MPa)	18	–
	2 days compression (MPa)	31	20 min.
	7 days compression (MPa)	41	–
	28 days compression (MPa)	57	42–62
Additional	Heat of hydration (J/g)	300	
	C3A	3	5 max.
	C3A + C4AF	17	22 max.

Table 2
Immersion time of mortar samples in salt water.

Sample	Time Submerged
MM1-00-5 (BLANK)	Not submerged
MM2-03-5	3 months
MM3-09-5	9 months
MM4-30-5	30 months

the LIBS analysis for the study of chloride penetration.

2.2. LIBS parameters

In previous work, optimization of LIBS measurements was performed [55]. Thus, the best gas pressure and composition conditions for the plasma creation leading to more reliable LIBS results were identified. In the present work, measurements were taken under those (optimized)
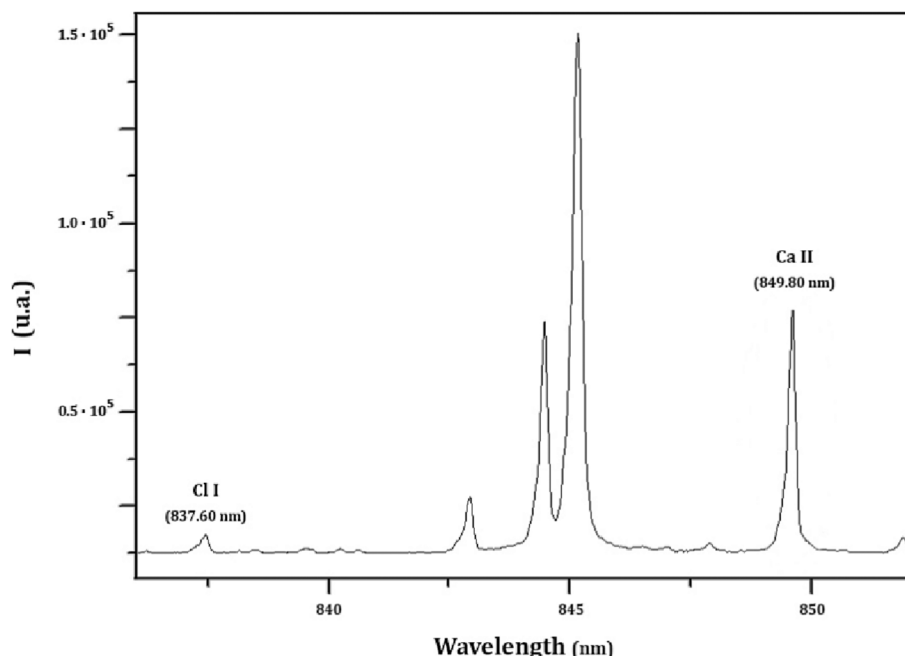

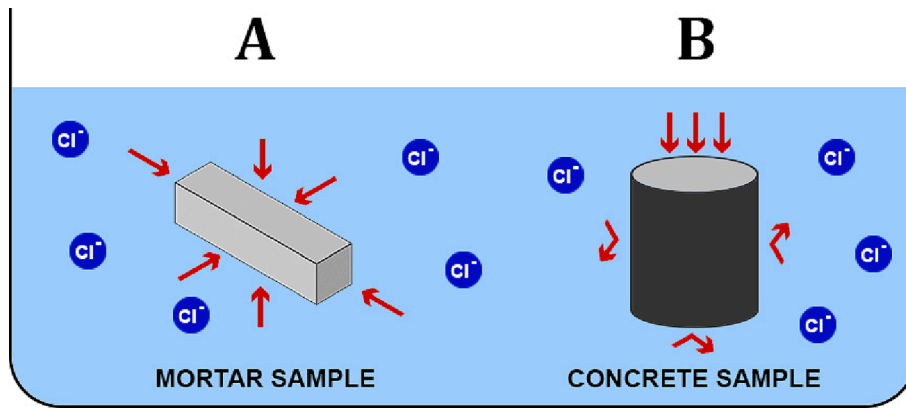**Fig. 2.** Typical spectrum showing Cl I 837.60 nm and Ca II 849.80 nm lines.

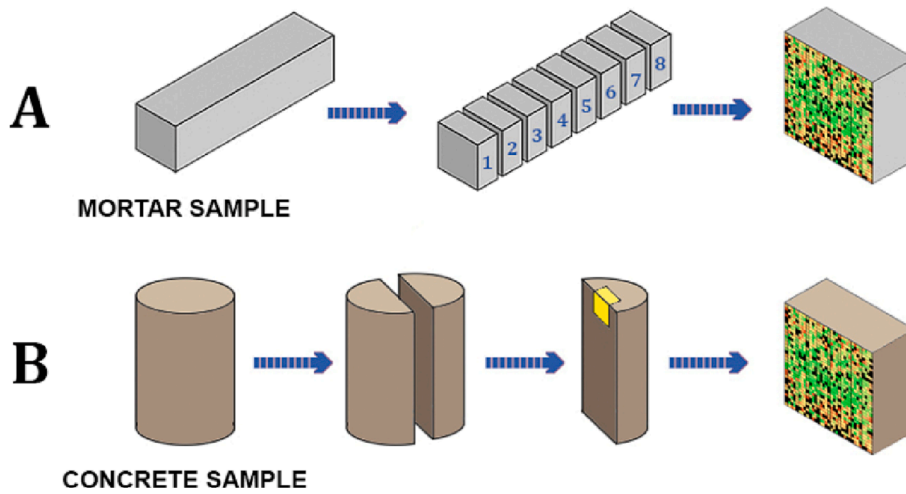**Fig. 3.** Submerged samples in salt-saturated water.

Fig. 4. Slicing procedure of mortar and concrete samples.

experimental conditions. In this way, a helium atmosphere was kept inside the vacuum chamber (with a continuous helium flow) under a pressure of 1000 mbar. A delay of 700 ns between the laser pulse and spectra acquisition was set. The window opening time for the iCCD was 10 μs and 20 accumulations per measurement were taken.

2.3. Analysis and data processing

All samples were analyzed immediately after being sliced, so that the chemical composition of the areas of interest was preserved at all times, avoiding their exposure to external agents, and keeping them isolated until the moment of analysis. LIBS analysis was performed all over the entire surface of the sliced section of the sample, with a spatial resolution of 1.2 mm. Thus, the 40 × 40 mm^2 surface to be examined was covered by a grid of 33 × 33 cells, providing a result of 70 measurements/cm^2 (Fig. 5).

The calibration procedure previously done [55], establishing the relationship between the ratio of peak areas $I(Cl)/I(Ca)$ obtained from LIBS analysis and the concentration of chloride ion present in the samples (eq. (1)) was used:

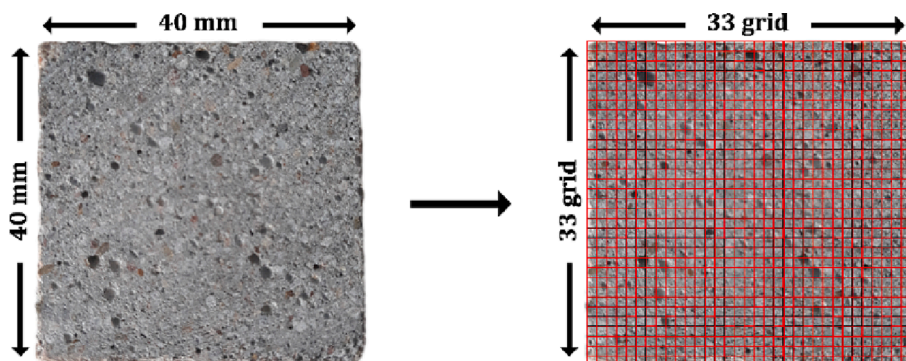$$I(Cl)/I(Ca) = 7.31 \bullet 10^{-3} + 13.69 \bullet 10^{-3} \bullet \%Cl^- \tag{1}$$

Fig. 5. Grid of 33x33 cells for the surface analysis of the samples.

This calibration procedure was validated by comparison with results from chemical analysis according to the method described in the EN 196–2:2013 standard [58].

Let us remark that, since the Ca II line depends on the composition of the cement used in the manufacture of the specimens, this calibration curve (**eq. (1)** can only be applied to samples composed of cement with similar calcium proportions. For the analysis of samples made with other types of cement, a new calibration would be necessary (Fig. 6).

3. Results

3.1. LIBS analysis of the submerged mortar samples

Results from the surface analysis show the chloride ion distribution in the samples. Thus, the ion penetration profiles and their variation with depth are shown in detail in Fig. 7. The black dots correspond to regions where the siliceous phase predominates (free from chloride ions), whereas parts with high chloride ion concentration correspond to zones where penetration is favored. As shown, chloride ions distribute with higher concentrations on the superficial zones of the sample and progressively advance towards the center, which becomes gradually more populated with chloride ions as the immersion time increases.

Averaged values of chloride ions were obtained from the 1089 surface measurements corresponding to 33×33 grids. The averaged concentrations obtained from LIBS analysis for the different mortar samples are gathered in Table 3.

Regarding the influence of the immersion periods, it can be seen in Fig. 8 that a remarkable increase in the average concentration of chloride ions takes place during the first stages of immersion, which gradually slows down as the immersion time increases until reaching a maximum limit for very long immersion periods.

These results allow us to get some details about the diffusion of Cl^- ions through mortar samples, considering that this process is governed by the Fick's laws. Indeed, the change in the concentration of ions over time ruled by Fick's second law given by the following expression:

$$\frac{\partial C}{\partial t} = D \frac{\partial^2 C}{\partial x^2} \tag{2}$$

where D is the effective diffusion coefficient, C is the concentration of

chloride ion and x is the variable position. Considering a constant chloride concentration at the exposed surface, and a constant diffusion coefficient the analytic solution to (**eq. (2)** is:

$$C_{x,t} = C_{x=0} + (C_{t=0} - C_{x=0})erf\left(\frac{x}{2\sqrt{Dt}}\right) \tag{3}$$

where $C_{x=0}$ is the ion chloride concentration at the surface and $C_{t=0}$ is the initial concentration, and erf the error function. From it, the effective diffusion coefficient of chloride ion in a material can be calculated by measuring the concentration at different depths [8–15,59–66].

In the present work, due to Cl^- evaporation near the surface taking place upon taking out the sample from salted water, Fick's second law only applies from a depth x_0. Accordingly, (**eq. (3)** can be rewritten as:

$$C_{x,t} = C_{x=0} + (C_{t=0} - C_{x=0})erf\left(\frac{x - x_0}{2\sqrt{Dt}}\right) \tag{4}$$

The average concentration of Cl^- ions was calculated for each depth position by integration considering its distance to the surface. A representation of this average concentration versus depth for each sample is shown in Fig. 9 **a-c**. By fitting these measurements to the theoretical behavior expressed by (**eq. (4)**, parameters $C_{x=0}$, $C_{t=0}$, D, and x_0 of the mortar samples studied were obtained (see Table 4).

Interestingly, the initial concentration of chloride ions in the sample $C_{t=0}$ was not cero, indicating that a primary and relatively fast transport of chloride ions from the surface towards the central zone of the sample took place at the earlier stages. We tentatively attribute this fact to adsorption phenomenon which should be playing an outstanding role in these mortars due to their porosity [7,8,59,66]. In this way, the solution containing Cl^- ions would have advanced by capillary suction towards the mortar sample center from all their lateral faces. This process would have taken place in a short lapse of time (compared to typical diffusion times), favored by the small size of the sample. In a longer scale of time, chloride ions diffusion through the matrix of the material would take place.

On the other hand, the difference in the measured values of x_0 can be attributed to the different time intervals that elapsed from the moment the samples were removed from the saline solution and the moment the LIBS measurements were made.
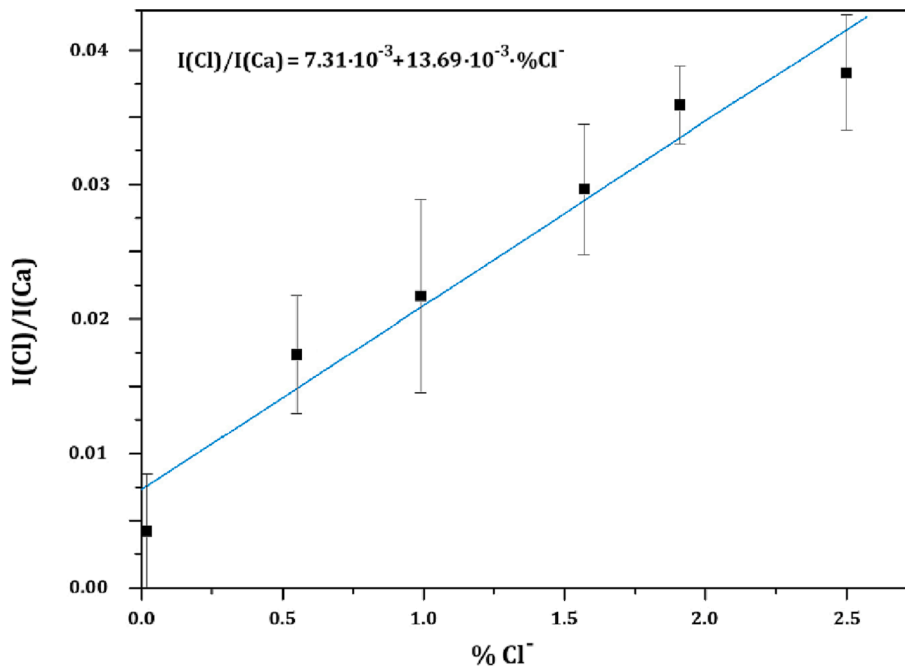

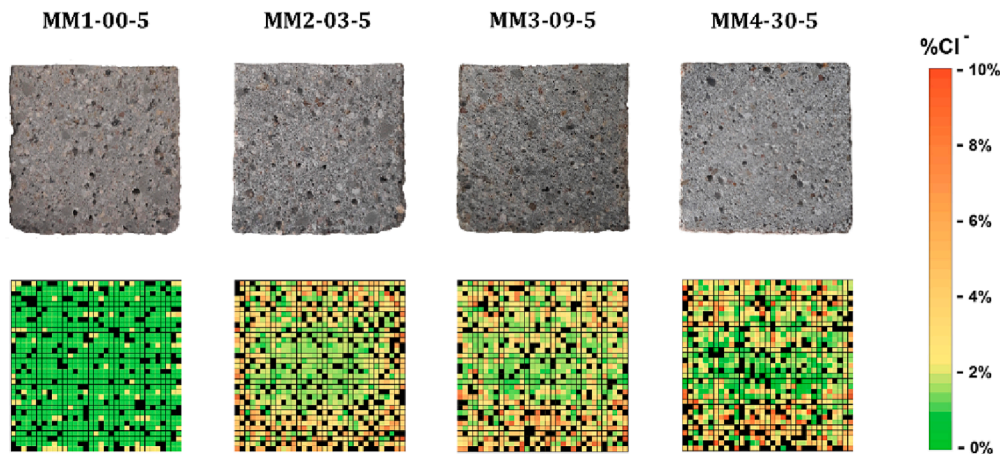**Fig. 6.** Calibration curve for I (Cl)/I(Ca) ratio vs Cl^- concentration.

Fig. 7. Results of LIBS surface analysis on submerged mortar samples.

Table 3
Average %Cl⁻ of mortar samples in salt water.

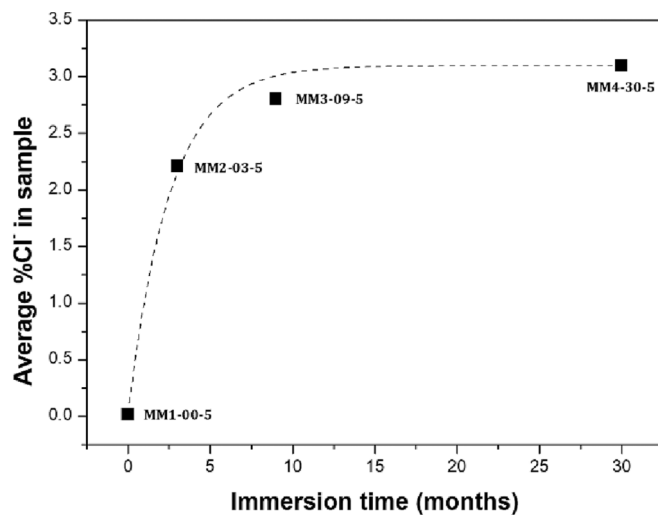| Sample	Average %Cl⁻
MM1-00-5 (BLANK)	0.0157
MM2-03-5	2.2093
MM3-09-5	2.8020
MM4-30-5	3.0957

Fig. 8. Average %Cl⁻ for submerged mortar samples.

Subsequently, we obtained the following apparent diffusion coefficient values: $D_{3months} = (5.94 \pm 0.05) \times 10^{-13}$ m^2/s; $D_{9months} = (3.6 \pm 0.6) \times 10^{-13}$ m^2/s; $D_{30months} = (2.1 \pm 0.8) \times 10^{-13}$ m^2/s. These values are in the range of the values found in other similar studies (from 10^{-12} to 10^{-13} m^2/s) [10,12–15,59,61,62,65]. Fig. 10 represents these values over the immersion time, showing that an increase in the exposure time leads to a decrease in the diffusion coefficient. This time dependency of the apparent diffusion coefficient values has been reported by other authors [10,12,59,62,63,65,66] and follows the empirical expression:

$$D(t) = D_0(t_0/t)^{\alpha} \qquad (5)$$

being D_0 the initial diffusion coefficient after time t_0 and α the so-called *age-factor* of the material [62,63,65]. Different phenomena could be causing this decreasing of D, including the cement paste hydration and the porous tightening of the surface in contact with the salt water [65].

In this work, the α measured was 0.449 ± 0.006, in good agreement with the typical values of this parameter [65].

3.2. LIBS analysis of the submerged concrete sample

In the case of the concrete samples, the presence of large areas of aggregate hinders the homogeneous distribution of chloride ions. After sixty months of immersion, a large concentration of chloride ions can be observed in the area in direct contact with seawater, and this concentration decreases towards the interior of the sample (Fig. 11).

The average concentration of Cl⁻ ions was calculated for each depth position by integration considering its distance to the exposed upper surface (Fig. 12). Again, the experimental behavior fits reasonably well to the theoretical one given by (eq. (4). The parameters $C_{x=0}$, $C_{t=0}$, D, and x_0 obtained in this case are gathered in Table 5.

As expected, $C_{t=0}$ value was approximately cero. Indeed, the high compactness of the concrete made it negligible the initial adsorption mechanism present in the small mortar samples.

On the other hand, the apparent diffusion coefficient in this case was $D_{60months} = (1.81 \pm 0.03) \times 10^{-13}$ m^2/s (see Fig. 10). Although this value of the diffusion coefficient cannot be compared to previous mortar ones because the compaction energy used in the manufacture of the concrete specimens was higher than that used with the mortar (which also contributes to increasing the material resistance to the diffusion of elements through it) and the different experimental designs, Fig. 10 shows that it is not long from the time trend found for mortar.

4. Final remarks

Laser-induced breakdown spectroscopy has become a widely used tool for analysis in numerous applications. Its use for diagnosis of the degradation state of construction materials, and in particular for the analysis of chloride concentration, provides several advantages over other techniques traditionally used. As shown in this work, this technique allows to obtain a high-resolution mapping of the chloride ions distribution in these type of materials with minimal sample spoilage. Both features made LIBS particularly appropriate for the study of chloride diffusion and corrosion in construction materials being exposed to salted environments, including mortar and concrete. The suitability of this technique for this application has been thoughtfully studied for the first time in this work.

Several mortar samples were subjected to the action of the chloride ion for different periods of time (3, 9, and 30 months), and the penetration through the material was studied, obtaining a full picture of chlorides diffusion inside these samples using LIBS.

The chloride ion concentrations at different depths were measured and from them, the mechanisms governing Cl⁻ penetration in the
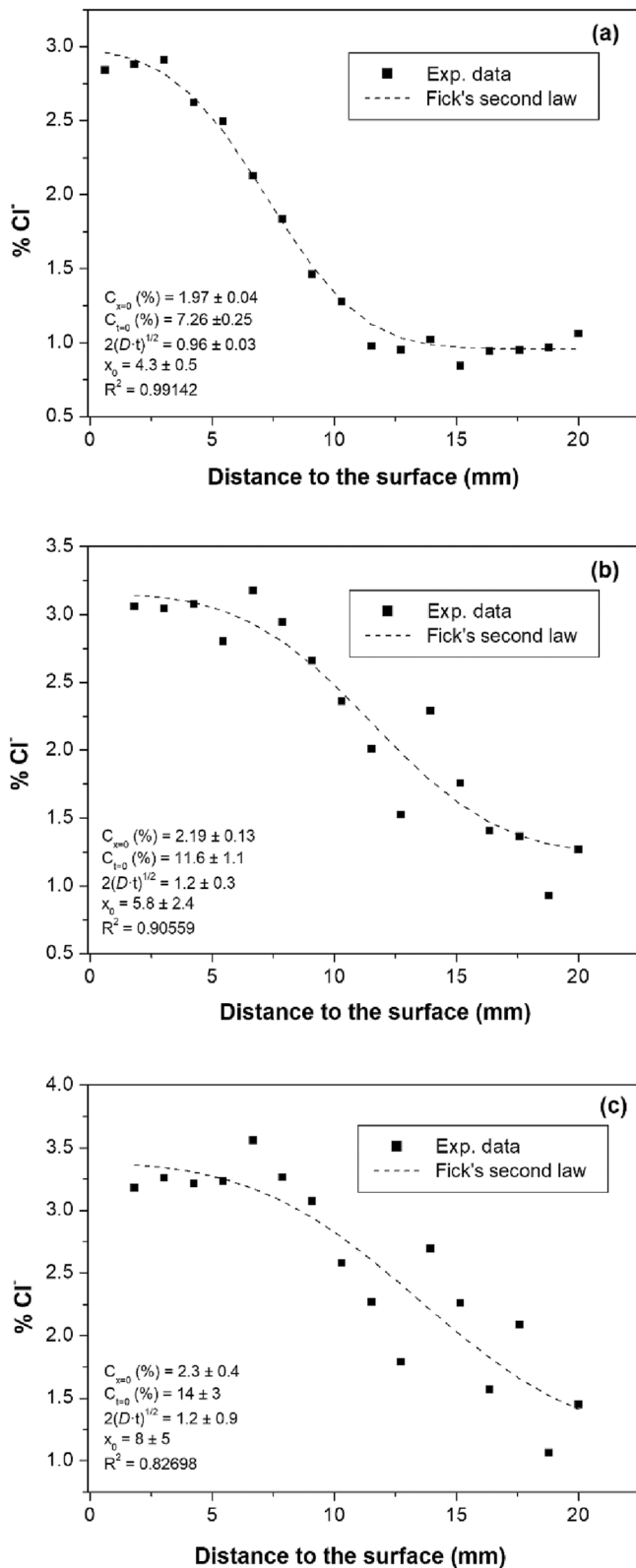
Fig. 9. Averaged Cl⁻ concentration (in %) at different distances from the surface for mortar samples.

Table 4
Diffusion parameters values for mortar samples.

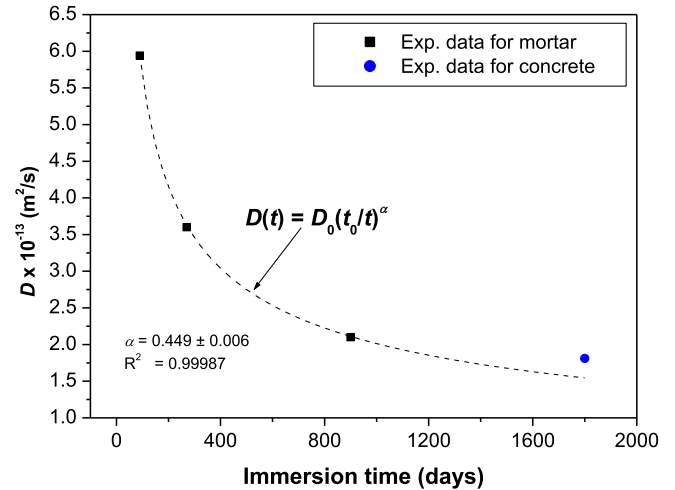| t (months)	$C_{x=0}$ (%)	$C_{t=0}$(%)	$2\sqrt{Dt}$(mm)	x_0(mm)
3	1.97 ± 0.04	0.96 ± 0.03	4.3 ± 0.5	7.26 ± 0.25
9	2.19 ± 0.13	1.2 ± 0.3	5.8 ± 2.4	11.6 ± 1.1
30	2.3 ± 0.4	1.2 ± 0.9	8 ± 5	14 ± 3

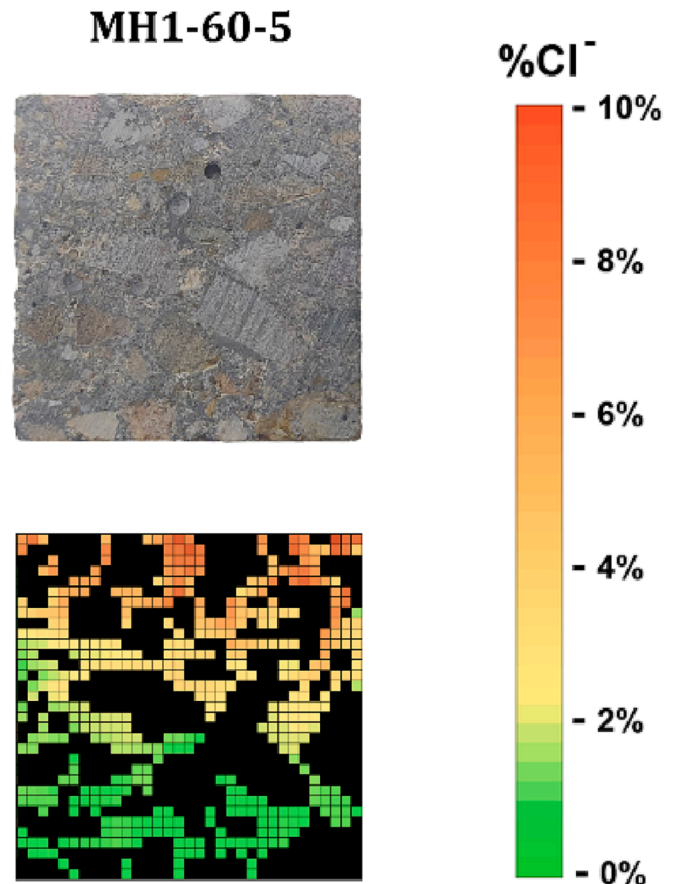**Fig. 10.** Dependence of the apparent diffusion coefficient with sample immersion time.

Fig. 11. Results of LIBS surface analysis on the submerged concrete sample.

samples have been elucidated. Thus, the results from this work have shown that chloride diffusion fits Fick's second law with an initial concentration, accounting for a primary and relatively fast transport of chloride ions from the surface towards the center of the sample taking place at the earlier stages (likely due to their high porosity). Also, this
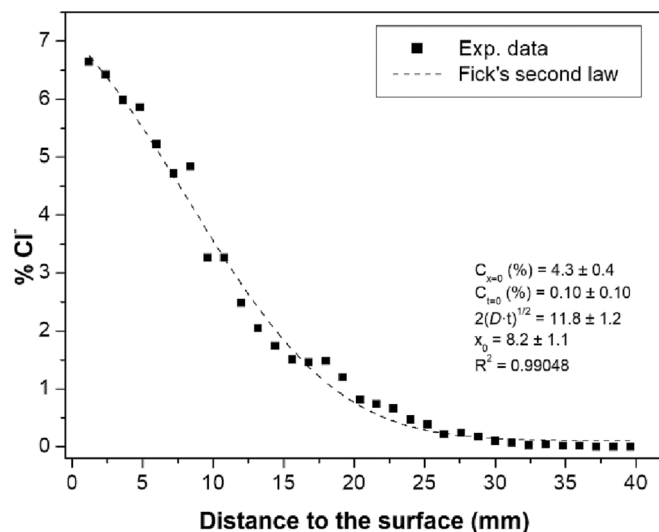
Fig. 12. Averaged Cl^- concentration (in %) at different distances from the surface for concrete sample.

Table 5
Diffusion parameter values for the concrete sample.

t (months)	$C_{x=0}$ (%)	$2\sqrt{Dt}$ (mm)	$C_{t=0}$ (%)	x_0 (mm)
60	4.3 ± 0.4	11.8 ± 1.2	0.1 ± 0.1	8.2 ± 1.10

technique has proved that some evaporation of Cl^- ions took place on the surface of the sample.

From Fick's second law, the apparent diffusion coefficient D was determined for the three mortar samples. The values measured for this parameter are in the order of 10^{-13} m^2/s, agreeing with results found in similar studies. It was also demonstrated that the immersion time evolution of D follows the empirical $t^{-\alpha}$ dependency, with an age-factor $\alpha = 0.449 \pm 0.006$, in good agreement with other authors' results.

Finally, LIBS was also applied to a concrete sample submitted to a 60-months-long period of immersion in the salt-saturated solution. The presence of large aggregates in this sample precluded the homogeneous distribution of chloride ions. A D in the order of 10^{-13} m^2/s was obtained.

In summary, results from this work have shown that LIBS is a promising technique for the study of chloride ion diffusion in construction materials. A more detailed analysis exploring other experimental conditions (including bigger samples and shorter immersion times, among others), will be the subject of future work in order to investigate in more detail how penetration takes place at the earlier stages.

CRediT authorship contribution statement

J. Mateo: Data curation, Investigation, Methodology, Writing – original draft. **M.C. García:** Formal analysis, Investigation, Supervision, Writing – review & editing. **A. Rodero:** Conceptualization, Formal analysis, Investigation, Methodology, Supervision, Writing – review & editing.

Declaration of Competing Interest

The authors declare that they have no known competing financial interests or personal relationships that could have appeared to influence the work reported in this paper.

Data availability

Data will be made available on request.

References

[1] Fortune Business Insights. *Ready-mix concrete market size, share & COVID-19 impact analysis, by application (residential, commercial, and infrastructure), and regional forecast, 2021-2028.* https://www.fortunebusinessinsights.com/ready-mix-concrete-market-103281 (2021).

[2] X. Shi, N. Xie, K. Fortune, J. Gong, Durability of steel reinforced concrete in chloride environments: an overview, Constr. Build. Mater. 30 (2012) 125–138, https://doi.org/10.1016/j.conbuildmat.2011.12.038.

[3] U. Angst, B. Elsener, C.K. Larsen, Ø. Vennesland, Chloride induced reinforcement corrosion: electrochemical monitoring of initiation stage and chloride threshold values, Corros. Sci. 53 (2011) 1451–1464, https://doi.org/10.1016/j.corsci.2011.01.025.

[4] P. Ghods, O.B. Isgor, G.A. McRae, G.P. Gu, Electrochemical investigation of chloride-induced depassivation of black steel rebar under simulated service conditions, Corros. Sci. 52 (2010) 1649–1659, https://doi.org/10.1016/j.corsci.2010.02.016.

[5] H.S. Wong, Y.X. Zhao, A.R. Karimi, N.R. Buenfeld, W.L. Jin, On the penetration of corrosion products from reinforcing steel into concrete due to chloride-induced corrosion, Corros. Sci. 52 (2010) 2469–2480, https://doi.org/10.1016/j.corsci.2010.03.025.

[6] Y. Tian, C. Dong, X. Cheng, Y. Wan, G. Wang, K. Xiao, X. Li, The micro-solution electrochemical method to evaluate rebar corrosion in reinforced concrete structures, Constr. Build. Mater. 151 (2017) 607–614, https://doi.org/10.1016/j.conbuildmat.2017.06.003.

[7] R.F. Feldman, Diffusion measurements in cement paste by water replacement using Propan-2-ol, Cem. Concr. Res. 17 (1987) 602–612, https://doi.org/10.1016/0008-8846(87)90133-5.

[8] P. Halamickova, R.J. Detwiler, D.P. Bentz, E.J. Garbockzi, Water permeability and chloride ion diffusion in Portland cement mortars: relationship to sand content and critical pore diameter, Cem. Concr. Res. 25 (1995) 790–802, https://doi.org/10.1016/0008-8846(95)00069-O.

[9] M. Shakouri, N.P. Vaddey, D. Trejo, Effect of admixed and external chlorides on transport of chlorides in concrete, ACI Mater. J. 116 (2019) 119–128. https://doi.org/10.14359/51716833.

[10] P.S. Mangat, O.O. Ojedokun, Free and bound chloride relationships affecting reinforcement cover in alkali activated concrete, Cem. Concr. Compos. 112 (2020) 103692, https://doi.org/10.1016/j.cemconcomp.2020.103692.

[11] D. Li, L.-Y. Li, X. Wang, Chloride diffusion model for concrete in marine environment with considering binding effect, Mar. Struct. 66 (2019) 44–51, https://doi.org/10.1016/j.marstruc.2019.03.004.

[12] Y. Wang, X. Gong, L. Wu, Prediction model of chloride diffusion in concrete considering the coupling effects of coarse aggregate and steel reinforcement exposed to marine tidal environment, Constr. Build. Mater. 216 (2019) 40–57, https://doi.org/10.1016/j.conbuildmat.2019.04.221.

[13] M. Cabeza, B. Díaz, X.R. Nóvoa, C. Pérez, M.C. Pérez, The effect of loading on the diffusivity of chlorides in mortar, Materials 12 (2019) 2527–2539, https://doi.org/10.3390/ma12162527.

[14] X.-H. Wang, L. Zheng, Effect of different pre-exposure loading on chloride penetration in reinforced concrete specimens, Int. J. Civ. Eng. 17 (2019) 1075–1094, https://doi.org/10.1007/s40999-018-0359-z.

[15] B. Yu, Q. Ma, H.-C. Huang, Z. Chen, Probabilistic prediction model for chloride diffusion coefficient of concrete in terms of material parameters, Constr. Build. Mater. 215 (2019) 941–957, https://doi.org/10.1016/j.conbuildmat.2019.04.147.

[16] F. Du, Z. Jin, C. Xiong, Y. Yu, J. Fan, Effects of transverse crack on chloride ions diffusion and steel bars corrosion behavior in concrete under electric acceleration, Materials 12 (2019) 2481–2501, https://doi.org/10.3390/ma12152481.

[17] L.J. Radziemski, From LASER to LIBS, the path of technology development, Spectrochim. Acta B 57 (2002) 1109–1113, https://doi.org/10.1016/S0584-8547(02)00052-6.

[18] J. El Haddad, L. Canioni, B. Bousquet, Good practices in LIBS analysis: review and advices, Spectrochim. Acta B 101 (2014) 171–182, https://doi.org/10.1016/j.sab.2014.08.039.

[19] D.W. Hahn, N. Omenetto, Laser-induced breakdown spectroscopy (LIBS), part I: review of basic diagnostics and plasma-particle interactions: still-challenging issues within the analytical plasma community, Appl. Spectrosc. 64 (2010) 335–366, https://doi.org/10.1366/000370210793561691.

[20] Anna P.M. Michel, *Review: Applications of single-shot laser-induced breakdown spectroscopy*, Spectrochim. Acta B 65 (2010) 185-191. https://doi.org/10.1016/j.sab.2010.01.006.

[21] R. Ahmed, M.A. Baig, A comparative study of enhanced emission in double pulse laser induced breakdown spectroscopy, Opt. Laser Technol. 65 (2015) 113–118, https://doi.org/10.1016/j.optlastec.2014.07.011.

[22] F. Colao, V. Lazic, R. Fantoni, S. Pershin, A comparison of single and double pulse laser-induced breakdown spectroscopy of aluminum samples, Spectrochim. Acta B 57 (2002) 1167–1179, https://doi.org/10.1016/S0584-8547(02)00058-7.

[23] L. St-Onge, M. Sabsabi, P. Cielo, Analysis of solids using laser-induced plasma spectroscopy in double-pulse mode, Spectrochim. Acta B 53 (1998) 407–415, https://doi.org/10.1016/S0584-8547(98)00080-9.

[24] V.I. Babushok, F.C. DeLucia Jr., J.L. Gottfried, C.A. Munson, A.W. Miziolek, Double pulse laser ablation and plasma: Laser induced breakdown spectroscopy signal enhancement, Spectrochim. Acta B 61 (2006) 999–1014, https://doi.org/10.1016/j.sab.2006.09.003.

[25] S.M. Angel, D.N. Stratis, K.L. Eland, T. Lai, M.A. Berg, D.M. Gold, *LIBS using dual- and ultra-short laser pulses*, Fresen J. Anal. Chem. 369 (2001) 320–327, https://doi.org/10.1007/s002160000656.

[26] G. Nicolodelli, G.S. Senesi, R.A. Romano, I.L. Perazzoli, D.M. Milori, Signal enhancement in collinear double-pulse laser-induced breakdown spectroscopy applied to different soils, Spectrochim. Acta B 111 (2015) 23–29, https://doi.org/10.1016/j.sab.2015.06.008.

[27] O. Ayed Nassef, H.E. Elsayed-Ali, Spark discharge assisted laser induced breakdown spectroscopy, Spectrochim. Acta B 60 (2005) 1564–1572, https://doi.org/10.1016/j.sab.2005.10.010.

[28] L. Nagli, M. Gaft, Combining laser-induced breakdown spectroscopy with molecular laser-induced fluorescence, Appl. Spectrosc. 70 (2016) 585–592, https://doi.org/10.1177/0003702816631292.

[29] M. Bonta, J.J. Gonzalez, C.D. Quarles Jr., R.E. Russo, B. Hegedus, A. Limbeck, Elemental mapping of biological samples by the combined use of LIBS and LA-ICP-MS, J. Anal. Atom Spectrom. 31 (2016) 252–258, https://doi.org/10.1039/c5ja00287g.

[30] L. Brunnbauer, M. Mayr, S. Larisegger, M. Nelhiebel, L. Pagnin, R. Wiesinger, M. Schreiner, A. Limbeck, Combined LA-ICP-MS/LIBS: powerful analytical tools for the investigation of polymer alteration after treatment under corrosive conditions, Sci. Rep. 10 (2020) 12513, https://doi.org/10.1038/s41598-020-69210-9.

[31] R. Noll, V. Sturm, Ü. Aydin, D. Eilers, C. Gehlen, M. Höhne, A. Lamott, J. Makowe, J. Vrenegor, Laser-induced breakdown spectroscopy – From research to industry, new frontiers for process control, Spectrochim. Acta B 63 (2008) 1159–1166, https://doi.org/10.1016/j.sab.2008.08.011.

[32] R. Noll, C. Fricke-Begemann, M. Brunk, S. Connemann, C. Meinhardt, M. Scharun, V. Sturm, J. Makowe, C. Gehlen, Laser-induced breakdown spectroscopy expands into industrial applications, Spectrochim. Acta B 93 (2014) 41–51, https://doi.org/10.1016/j.sab.2014.02.001.

[33] D.W. Hahn, N. Omenetto, Laser-induced breakdown spectroscopy (LIBS), part II: review of instrumental and methodological approaches to material analysis and applications to different fields, Appl. Spectrosc. 66 (2012) 347–419, https://doi.org/10.1366/11-06574.

[34] S. Guirado, F.J. Fortes, J.J. Laserna, Elemental analysis of materials in an underwater archeological shipwreck using a novel remote laser-induced breakdown spectroscopy system, Talanta 137 (2015) 182–188, https://doi.org/10.1016/j.talanta.2015.01.033.

[35] J. Serrano, J. Moros, C. Sánchez, J. Macías, J.J. Laserna, Advanced recognition of explosives in traces on polymer surfaces using LIBS and supervised learning classifiers, Anal. Chim. Acta 806 (2014) 107–116, https://doi.org/10.1016/j.aca.2013.11.035.

[36] M. Akhtar, A. Jabbar, S. Mehmood, N. Ahmed, R. Ahmed, M.A. Baig, Magnetic field enhanced detection of heavy metals in soil using laser induced breakdown spectroscopy, Spectrochim. Acta B 148 (2018) 143–151, https://doi.org/10.1016/j.sab.2018.06.016.

[37] T. Wang, M. He, T. Shen, F. Liu, Y. He, X. Liu, Z. Qiu, Multi-element analysis of heavy metal content in soils using laser-induced breakdown spectroscopy: a case study in eastern China, Spectrochim. Acta B 149 (2018) 300–312, https://doi.org/10.1016/j.sab.2018.09.008.

[38] E.C. Ferreira, E.J. Ferreira, P.R. Villas-Boas, G.S. Senesi, C.M. Carvalho, R. A. Romano, L. Martin-Neto, D.M. Milori, Novel estimation of the humification degree of soil organic matter by laser-induced breakdown spectroscopy, Spectrochim. Acta B 99 (2014) 76–81, https://doi.org/10.1016/j.sab.2014.06.016.

[39] S. Moncayo, S. Manzoor, T. Ugidos, F. Navarro-Villoslada, J.O. Caceres, Discrimination of human bodies from bones and teeth remains by laser induced breakdown spectroscopy and neural networks, Spectrochim. Acta B 101 (2014) 21–25, https://doi.org/10.1016/j.sab.2014.07.008.

[40] G. Bilge, I.H. Boyaci, K.E. Eseller, U. Tamer, S. Çakir, Analysis of bakery products by laser-induced breakdown spectroscopy, Food Chem. 181 (2015) 186–190, https://doi.org/10.1016/j.foodchem.2015.02.090.

[41] M. Markiewicz-Keszycka, X. Cama-Moncunill, M.P. Casado-Gavalda, Y. Dixit, R. Cama-Moncunill, P.J. Cullen, C. Sullivan, Laser-induced breakdown spectroscopy (LIBS) for food analysis: a review, Trends Food Sci. Technol. 65 (2017) 80–93, https://doi.org/10.1016/j.tifs.2017.05.005.

[42] H. Zheng, F.Y. Yueh, T. Miller, J.P. Singh, K.E. Zeigler, J.C. Marra, Analysis of plutonium oxide surrogate residue using laser-induced breakdown spectroscopy, Spectrochim. Acta B 63 (2008) 968–974, https://doi.org/10.1016/j.sab.2008.06.005.

[43] H. Sobral, R. Sanginés, A. Trujillo-Vázquez, Detection of trace elements in ice and water by laser-induced breakdown spectroscopy, Spectrochim. Acta B 78 (2012) 62–66, https://doi.org/10.1016/j.sab.2012.09.005.

[44] X. Wang, V. Motto-Ros, G. Panczer, D. De Ligny, J. Yu, J.M. Benoit, J.L. Dussossoy, S. Peuget, Mapping of rare earth elements in nuclear waste glass-ceramic using micro laser-induced breakdown spectroscopy, Spectrochim. Acta B 87 (2013) 139–146, https://doi.org/10.1016/j.sab.2013.05.022.

[45] Y. Yu, W. Zhou, X. Su, Detection of Cu in solution with double pulse laser-induced breakdown spectroscopy, Opt. Commun. 333 (2014) 62–66, https://doi.org/10.1016/j.optcom.2014.07.053.

[46] Y.-S. Kim, B.-Y. Han, H.S. Shin, H.D. Kim, E.C. Jung, J.H. Jung, S.H. Na, Determination of uranium concentration in an ore sample using laser-induced breakdown spectroscopy, Spectrochim. Acta B 74–75 (2012) 190–193, https://doi.org/10.1016/j.sab.2012.06.029.

[47] B. Savija, E. Schlangen, J. Pacheco, S. Millar, T. Eichler, G. Wilsch, Chloride ingress in cracked concrete: a laser induced breakdown spectroscopy (LIBS) study, J. Adv. Concr. Technol. 12 (2014) 425–442, https://doi.org/10.3151/jact.12.425.

[48] S. Eto, T. Matsuo, T. Matsumura, T. Fujii, M.Y. Tanaka, Quantitative estimation of carbonation and chloride penetration in reinforced concrete by laser-induced breakdown spectroscopy, Spectrochim. Acta B 101 (2014) 245–253, https://doi.org/10.1016/j.sab.2014.09.004.

[49] G. Ebell, A. Burkert, T. Günther, G. Wilsch, Determination of the corrosion-inducing chloride content of stainless ferritic reinforcing steels in mortar, Bautechnik 97 (2020) 21–31, https://doi.org/10.1002/bate.201900077.

[50] G. Wilsch, F. Weritz, D. Schaurich, H. Wiggenhauser, Determination of chloride content in concrete structures with laser-induced breakdown spectroscopy, Constr. Build. Mater. 19 (2005) 724–730, https://doi.org/10.1016/j.conbuildmat.2005.06.001.

[51] S. Millar, S. Kruschwitz, G. Wilsch, Determination of total chloride content in cement pastes with laser-induced breakdown spectroscopy (LIBS), Cem. Concr. Res. 117 (2019) 16–22, https://doi.org/10.1016/j.cemconres.2018.12.001.

[52] T.A. Labutin, A.M. Popov, S.M. Zaytsev, N.B. Zorov, M.V. Belkov, V.V. Kiris, S. N. Raikov, Determination of chlorine, sulfur and carbon in reinforced concrete structures by double-pulse laser-induced breakdown spectroscopy, Spectrochim. Acta B 99 (2014) 94–100, https://doi.org/10.1016/j.sab.2014.06.021.

[53] A.S. Bryukhova, A.A. Kuznetsov, I.V. Seliverstova, A.M. Popov, T.A. Labutin, N. B. Zorov, Evaluation of aging of reinforced concrete structures by laser-induced breakdown spectroscopy of reinforcement corrosion products, J. Appl. Spectrosc. 87 (2020) 800–804, https://doi.org/10.1007/s10812-020-01073-4.

[54] S. Millar, C. Gottlieb, T. Günther, N. Sankat, G. Wilsch, S. Kruschwitz, Chlorine determination in cement-bound materials with Laser-induced Breakdown Spectroscopy (LIBS) – A review and validation, Spectrochim. Acta B 147 (2018) 1–8, https://doi.org/10.1016/j.sab.2018.05.015.

[55] J. Mateo, M.C. Quintero, J.M. Fernández, M.C. García, A. Rodero, Application of LIBS technology for determination of Cl concentrations in mortar samples, Constr. Build. Mater. 204 (2019) 716–726, https://doi.org/10.1016/j.conbuildmat.2019.01.152.

[56] European Standard EN 196-1:2005, *Methods of testing cement. Determination of strength* (2005).

[57] European Standard EN 12390-2:2019, *Testing hardened concrete. Making and curing specimens for strength tests* (2019).

[58] European Standard EN 196-2:2013, *Methods of testing cement. Chemical analysis of cement* (2013).

[59] P.S. Mangat, O.O. Ojedokun, Bound chloride ingress in alkali activated concrete, Constr. Build. Mater. 212 (2019) 375–387, https://doi.org/10.1016/j.conbuildmat.2019.03.302.

[60] J. Liu, Y. Jia, J. Wang, Calculation of chloride ion diffusion in glass and polypropylene fiber-reinforced concrete, Constr. Build. Mater. 215 (2019) 875–885, https://doi.org/10.1016/j.conbuildmat.2019.04.246.

[61] X. Xie, Q. Feng, Z. Chen, L. Jiang, W. Lu, Diffusion and distribution of chloride ions in carbonated concrete with fly ash, Constr. Build. Mater. 218 (2019) 119–125, https://doi.org/10.1016/j.conbuildmat.2019.05.041.

[62] L.P. Tang, L.-O. Nilsson, Rapid determination of the chloride diffusivity in concrete by applying an electrical field, ACI Mater. J. 89 (1992) 40–53. https://doi.org/10.14359/1244.

[63] L. Song, W. Sun, J. Gao, Time dependent chloride diffusion coefficient in concrete, J. Wuhan Univ. Technol. 28 (2013) 314–319, https://doi.org/10.1007/s11595-013-0685-6.

[64] K. Takewaka, S. Mastumoto, Quality and cover thickness of concrete based on the estimation of chloride penetration in marine environments, ACI Mater. J. 109 (1988) 381–400. https://doi.org/10.14359/2124.

[65] G. Markeset, O. Skjølsvold, *Time dependent chloride diffusion coefficient - Field studies of concrete exposed to marine environment in Norway*. Proceedings of the 2nd International Symposium on Service Life Design for Infrastructure (2010).

[66] M. Fenaux (2013). *Ph.D. Thesis: Modelling of chloride transport in non-saturated concrete. From microscale to macroscale.* Universidad Politécnica de Madrid. https://doi.org/10.20868/UPM.thesis.1528.